

Melting and Pressure-Induced Amorphization of Quartz

James BADRO, Philippe GILLET and Jean-Louis BARRAT

December 2, 2024

It has recently been shown that amorphization and melting of ice [1] were intimately linked. In this letter, we infer from molecular dynamics simulations on the SiO_2 system that the extension of the α -quartz melting line in the metastable pressure-temperature domain is the pressure-induced amorphization line. It seems therefore likely that melting is the physical phenomenon responsible for pressure induced amorphization. Moreover, we show that the structure of a "pressure glass" is similar to that of a very rapidly (10^{13} to 10^{14} kelvins per second) quenched thermal glass.

Pressure induced amorphization (PIA) is an intriguing phenomenon. The first report of this transition goes back to 1984 when Mishima *et al.* [2] found that ice-Ih cooled down to 77 K and pressurized to 10 kbar failed to transform into crystalline Ice-IX and became amorphous. Since then, a large number of materials were found to undergo similar transitions [3] at different pressures and temperatures. In particular, quartz, one of the most studied minerals, was found to amorphize [4] at room temperature beginning about 22 GPa. A series of experiments [5, 6] and molecular dynamics (MD) simulations [7, 8, 9] have shown that this transition is accompanied by an increase in silicon coordination. However, the thermodynamic nature of this transition remains very poorly defined. It has been argued on the basis of lattice dynamics calculations [10] that the PIA of α -quartz takes place as the result of an elastic instability [11] occurring at approximately 22 GPa. Molecular dynamics calculations have confirmed the 22 GPa amorphisation threshold, but the role of the instability is still a matter of debate [12].

Hemley *et al.* [13] proposed that PIA of quartz represents the metastable extension of the melting curve of SiO_2 . Richet [14] using thermodynamical arguments has inferred that the vitrification upon room temperature *decompression* or upon room pressure heating of some high pressure silicate minerals represents crystal fusion. Recently, Mishima [1] has proposed that the pressure-induced transformation towards amorphous ice (high density amorphous phase) can be described as a melting transition to an extremely unrelaxed amorphous state. This state then slowly relaxes towards an energetically more favourable glass-like state. It has been shown using Raman spectroscopy that the amorphization induced by heating of stishovite leads to a highly unrelaxed glassy state [26, 3, 27] exhibiting the features of the pressure glass obtained upon room temperature compression and decompression of quartz¹, which then gradually transforms into a relaxed glassy state indistinguishable (at least from the vibrational point of view) from the usual thermal glass.

In this letter, we present results from molecular dynamics (MD) simulations that provide new insights into the relationship between PIA and melting, and on the structure of amorphous SiO_2 prepared by static compression of quartz at room temperature.

MD simulations have been used to investigate the melting and amorphization curves of α -quartz in the metastable P-T domain in which the nucleation of the high pressure polymorphs cannot be bypassed in laboratory experiments. Also, the cooling rates used for quenching liquid SiO_2 in MD simulations are by far larger than those used by current experimental techniques. MD calculations were carried out in an (N,P,T) isothermal-isobaric ensemble, for a system of 480 SiO_2 molecules. The BKS [15] pairwise interaction potential which has proven to provide a very accurate description of silica at high pressure [7, 16, 8], was used. A system in the α -quartz structure was subjected to compression at different temperatures, or to isochoric heating, until either amorphization or melting was observed. These amorphous states were detected

¹the reference pressure glasse we have modelized in this study

by a combined analysis of the radial distribution function and the energy jump at the transition, along with a plot of the average positions of the particles integrated on the duration of the simulation. The corresponding points are reported in the P-T phase diagram of figure 1. They represent only an estimate of a coexistence curve between the crystal, and the *melt* mainly because the system is highly non-ergodic and because the melting point is not calculated with the usual thermodynamic criteria. The term *melt* is used here for both the high temperature liquid state and the high pressure disordered state. Comparing these points with the experimental results for the melting of quartz, it seems clear that the amorphisation line is a reasonable extrapolation of the melting line. Calculation of the metastable extension of the equilibrium melting curve [13] have improved with the measurement of more thermodynamic data for the SiO₂ system [17]. The recent calculation by Zhang *et al.* [17] using the most recent thermodynamic data is quite close to the results obtained from the numerical simulation. Although the extrapolated pressures are lower than those in the simulation, these authors have argued that these curves can be shifted to higher pressures if corrected for the configurational entropy term arising from the distribution of four- five- and six-coordinated silicon ions in the *melt* at high pressure.

It should be noticed that the low-pressure (below 10 GPa) high-temperature calculated points differ from the experimental results, because melting in this non-ergodic region is inhibited by the very large viscosity of the liquid. This curve should therefore be corrected at lower pressure and should get closer to the experimental points of the equilibrium melting curve.

The continuity between PIA and melting should be reflected into some similarities between the structural and dynamical properties of the pressure amorphized material (thereafter called pressure glass) and of quenched liquids (thermal glasses). The properties of the latter type of systems are known to be sensitive to the quenching rate [18]. In order to compare pressure glasses and thermal glasses, we use as a reference state a sample of quartz, amorphized at 22 GPa, and then decompressed to room pressure, leading to a pressure glass with a density of $\rho = 3.07 \text{ g} \cdot \text{cm}^{-3}$. Thermal glasses were produced by cooling a high temperature liquid (7000 K) at room pressure and constant density $\rho = 2.2 \text{ g} \cdot \text{cm}^{-3}$ using three different cooling rates $\gamma = 4.4 \cdot 10^{12} \text{ K} \cdot \text{s}^{-1}$, $\gamma = 3.5 \cdot 10^{13} \text{ K} \cdot \text{s}^{-1}$ and $\gamma = 10^{15} \text{ K} \cdot \text{s}^{-1}$. These glassy systems were then compressed at 300 K to obtain densified glasses with densities of $\rho = 3.07 \text{ g} \cdot \text{cm}^{-3}$. A second set of thermal glasses was produced by cooling the high temperature liquid (7000 K) at a constant density of $\rho = 3.07 \text{ g} \cdot \text{cm}^{-3}$, with the same three cooling rates, to avoid the final compression step in a highly nonergodic system. Only the results relative to this last set of samples will be discussed below; similar, but less precise results were obtained with the samples cooled at $\rho = 2.2 \text{ g} \cdot \text{cm}^{-3}$.

Static and semi-dynamical quantities such as the coordination number distribution, ring statistics (figure 2) and vibrational densities of state (V-DOS, figure 3) were then calculated for these systems and compared to the corresponding quantities for the reference SiO₂ pressure glass.

The coordination distribution shows that the proportion of 4-coordinated Si species decreases with increasing cooling rates, whereas the proportion of 6-fold and especially 5-fold Si coordination rises.

The effect of the cooling rate on coordination distribution is consistent with the pressure dependence of the coordination distribution [19] in liquid SiO₂; as pressure rises in the 0–15 GPa range, the proportion of 4-fold coordinated Si species decreases whereas that of 5-fold (and in a lesser extent to 6-fold) coordinated Si species increases. The higher the cooling rate, the closer are the configurations of the supercooled and high temperature liquid (higher "fictive temperature"). The high temperature liquid at these densities is in a high pressure state, which is maintained during the quench resulting in the formation of a strongly frustrated amorphous state, because the application of such a high cooling rate "freezes" the system in such a short time compared with the mechanical relaxation time that the transformation is quasi-isochoric. These two observations represent two different pictures of the same phenomenon.

On the other hand, the ring statistics show that a high cooling rate reduces the proportion of the 5 and 6-membered rings characteristic of a low density structure in favour of small chains of 3-membered and 4-membered rings.

It has been proposed [20, 21] that the proportion of 3-membered and 4-membered rings increases with pressure in densified SiO₂ glass or pressure-induced amorphous quartz, on the basis of the concomitant intensity change of the Raman D₁ and D₂ defect lines associated with these rings [22, 23]. Our results for the cooling rate dependence of the ring statistics shows that the proportion of these clusters is also enhanced by higher cooling rates, showing that the maximum pressure (before decompression) attained during room temperature compression of quartz plays a role similar to that of the cooling rate during the quenching of a melt at room pressure.

The coordination distribution in the pressure glass is close to that of a thermal glass obtained with a cooling rate $\gamma \simeq 7 \cdot 10^{13} \text{ K} \cdot \text{s}^{-1}$ (fig. 2). The ring distribution displays the same characteristics, except for 6-membered rings whose proportions (within a few percent) are not very significant, due to the greater error bars in the determination of these larger scale structures in non-ergodic systems.

A similar conclusion can be drawn from the vibrational density of states (V-DOS, fig. 3); the high-frequency internal stretching modes for the SiO₄ units are strongly broadened in the pressure glass. This broadening is an increasing function of the cooling rates in the thermal glass. Another important feature is the peak at 900 cm⁻¹; the glasses with higher cooling rates have a narrower peak followed by a plateau, whereas glasses produced by slow cooling of the liquid show a broader peak followed by a drop in the V-DOS. Once again, the pressure glass exhibits a behaviour intermediate between that observed for the two rapidly cooled systems, and is very close to the glass cooled at $\gamma = 3.5 \cdot 10^{13} \text{ K} \cdot \text{s}^{-1}$. These results imply that the pressure glass has similar structural and thermodynamical properties as a rapidly cooled ($10^{13} \text{ K} \cdot \text{s}^{-1}$ to $10^{14} \text{ K} \cdot \text{s}^{-1}$) liquid at the same density and temperature. This supports the continuity between the liquid and the pressure glass, and therefore between the melting and the amorphisation curves.

A natural question is the relationship between our results and the possibility of a *polyamorphic* [24, 25] transition from a higher-entropy amorphous form of silica (the pressure glass) to a lower-entropy form (the thermal glass). In MD studies, there is no indication of any phase transition behaviour during densification, $\left(\frac{\partial P}{\partial V}\right)_T$ seems negative through the complete densification process at room temperature [7]. In order to accurately check the latter proposition, we carried out very long (N,P,T) simulations (0.134 nanoseconds) on SiO₂ glass cooled at $\gamma = 4.4 \cdot 10^{12} \text{ K} \cdot \text{s}^{-1}$ and compressed in the 5–15 GPa range. A histogram of the density fluctuations was then plotted and it showed a single yet broad maximum.

All these arguments concur with the fact that below T_g , the metastable extension of the quartz melting curve and the amorphization curve are identical. Metastable or thermodynamic melting can then be considered as the physical process responsible for high-pressure amorphization, at least in the case of silica and ice [1].

Acknowledgements

We wish to thank W. Kob for helpful comments and discussions, and especially for providing us with the initial systems for room pressure thermal glasses. We thank R.J. Hemley for helpful comments and discussions.

References

- [1] O. Mishima. *Nature*, **384**:546–549, 1996.
- [2] O. Mishima, L.D. Calvert, and E. Whalley. *Nature*, **310**:393–395, 1984.
- [3] P. Richet and Ph. Gillet. *Eur. J. Mineral.*, in press, 1997.
- [4] R.J. Hemley. In *High-Pressure research in mineral physics*, Mineral Physics 2. Terra Scientific Publishing Company – AGU, 1987.
- [5] C. Meade, R.J. Hemley, and H.K. Mao. *Phys. Rev. Lett.*, **69**:1387–1390, 1992.
- [6] J.-P. Iti, A. Polian, G. Calas, J. Petiau, A. Fontaine, and H. Tolentino. *Phys. Rev. Lett.*, **63**:389–401, 1989.
- [7] J.S. Tse and D.D. Klug. *Phys. Rev. Lett.*, **67**:3559, 1991.
- [8] J.S. Tse and D.D. Klug. *Science*, **255**:1559–1561, 1992.
- [9] N. Binggeli, N. Troullier, J.-L. Martins, and J.R. Chelikowsky. *Phys. Rev. B*, **44**:4471, 1991.

- [10] N. Binggeli and J.R. Chelikowsky. *Phys. Rev. Lett.*, **69**:2220–2223, 1992.
- [11] L.E. McNeil and M. Grimsditch. *Phys. Rev. Lett.*, **68**:83–85, 1992.
- [12] G.W. Watson and S.C. Parker. *Philosophical Mag. Lett.*, **71**:59–64, 1995.
- [13] R.J. Hemley, A.P. Jephcoat, H.K. Mao, L.C. Ming, and M.H. Manghnani. *Nature*, **334**:52–54, 1988.
- [14] P. Richet. *Nature*, **331**:56–58, 1988.
- [15] B.W.H. van Beest, G.J. Kramer, and R.A. van Santen. *Phys. Rev. Lett.*, **64**:1955–1958, 1990.
- [16] J. Badro, J.-L. Barrat, and Ph. Gillet. *Phys. Rev. Lett.*, **76**:772–775, 1996.
- [17] J. Zhang, R.C. Liebermann, T. Gasparik, and C.T. Herzberg. *J. Geophys. Research*, **98**:19785–19793, 1993.
- [18] K. Vollmayr, W. Kob, and K. Binder. *Phys. Rev. B*, **54**:15808–15827, 1996.
- [19] J.-L. Barrat, J. Badro, and Ph. Gillet. *J. Mol. Sim.*, Accepted, 1997.
- [20] R.J. Hemley, H.K. Mao, P.M. Bell, and B.O. Mysen. *Phys. Rev. Lett.*, **57**:747–750, 1986.
- [21] P.F. McMillan, B.T. Poe, Ph. Gillet, and B. Reynard. *Geochim. Cosmochim. Acta*, **58**:3653–3664, 1994.
- [22] R.J. Bell, N.F. Bird and P. Dean. *J. Phys. C*, **1**:299, 1968.
- [23] F.L. Galeener, A.J. Leadbetter and M.W. Stringfellow. *Phys. Rev. B*, **27**:1052, 1983.
- [24] P.H. Poole, T. Grande, F. Sciortino, H.E. Stanley, and C.A. Angell. *Comp. Mat. Sci.*, **223**:1–9, 1995.
- [25] S. Aasland and P.F. McMillan. *Nature*, **369**:663, 1994.
- [26] Ph. Gillet, A. Le Clac’h, and M. Madon. *J. Geophys. Res.*, **95**:21635–21655, 1990.
- [27] M. Grimsditch, S. Popova, V.V. Brazhkin, and R.N. Voloshin. *Phys. Rev. B*, **50**:12984–12986, 1994.

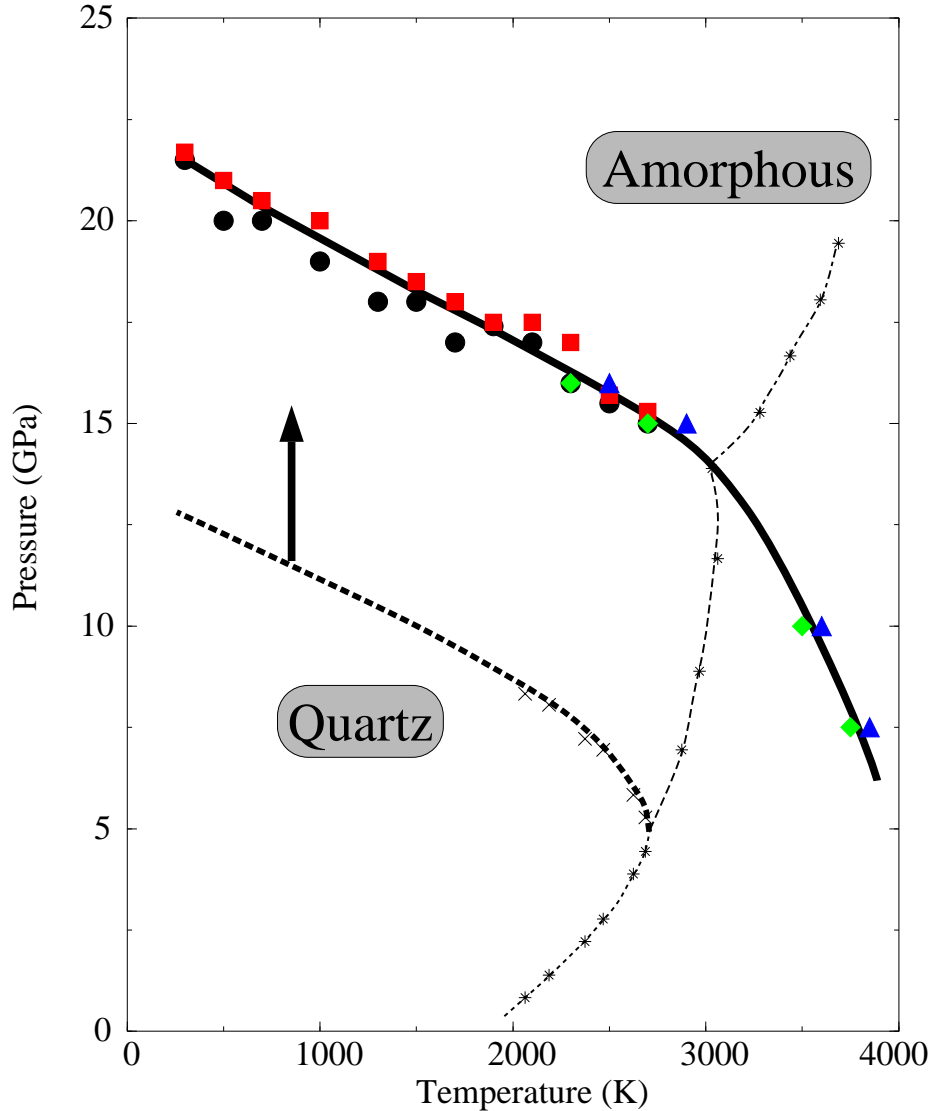


Figure 1: The quartz-melt coexistence curve (thick solid line). This line separates the phase diagram into two distinct areas: the quartz metastability field and the region where amorphous silica is more stable than quartz. The points represented by circles and squares represent the (vertical) error bars on the pressures needed to amorphize the system at constant temperature. In the same manner, the diamonds and triangles are the (horizontal) error bars on the temperatures needed to melt the system at constant pressure. It can be noticed that pressurization and heating points give the same results in the crossover region. The experimental points (stars) on the experimental equilibrium quartz (dotted), coesite (dashed) and stishovite (dot-dashed) melting lines are reported and the quartz melting curve is then extrapolated (thick dashed line) to higher pressures and lower temperatures using the measured thermodynamic data for quartz (data by Zhang *et al.* [17]). MD simulations are unable to estimate (within reasonable computation time limits) the correct temperatures of melting of solids whose liquid state is highly viscous (above 1 Pa.s), which is the case for SiO_2 at low pressure [19]. The arrow indicates that the extrapolated melting curve must be shifted to higher pressures in order to account for the presence of five and six-fold coordinated silicon species [17].

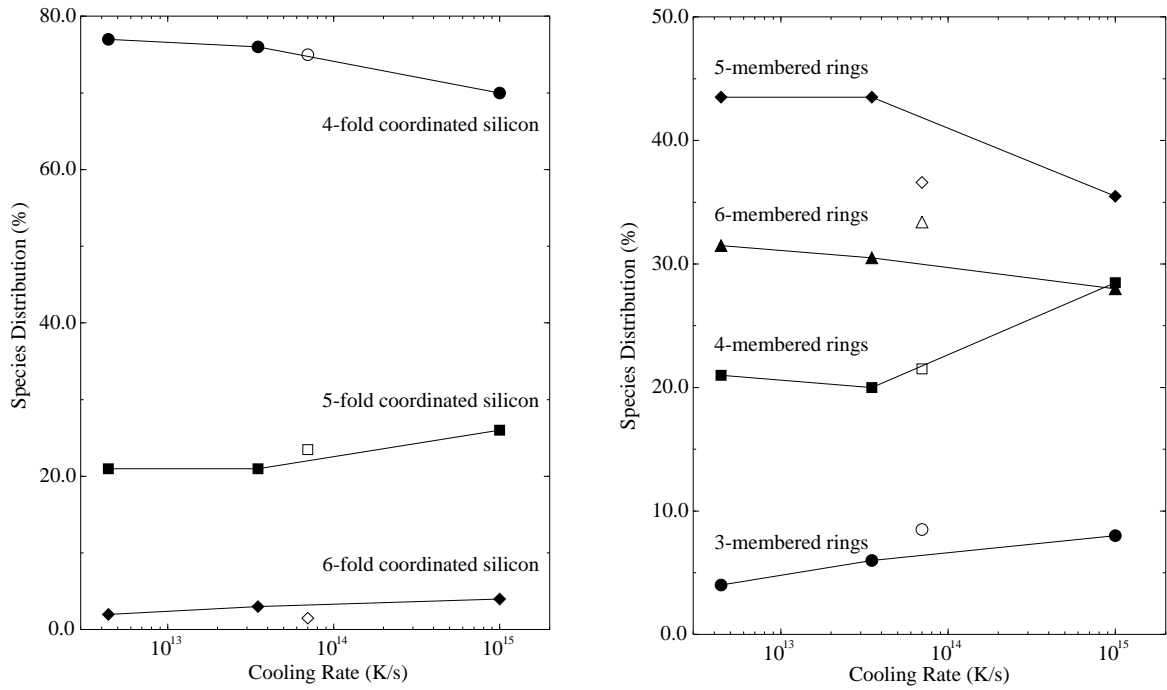


Figure 2: The structural properties of the glassy systems at $\rho = 3.07 \text{ g} \cdot \text{cm}^{-3}$ and 300 K. The coordination (left) and ring distributions (right) are reported for the three thermal glasses (filled symbols) as a function of their cooling rates. The corresponding quantities for the pressure glass (open symbols) are close to what would be obtained for a cooling rate $\gamma \simeq 7 \cdot 10^{13} \text{ K} \cdot \text{s}^{-1}$.

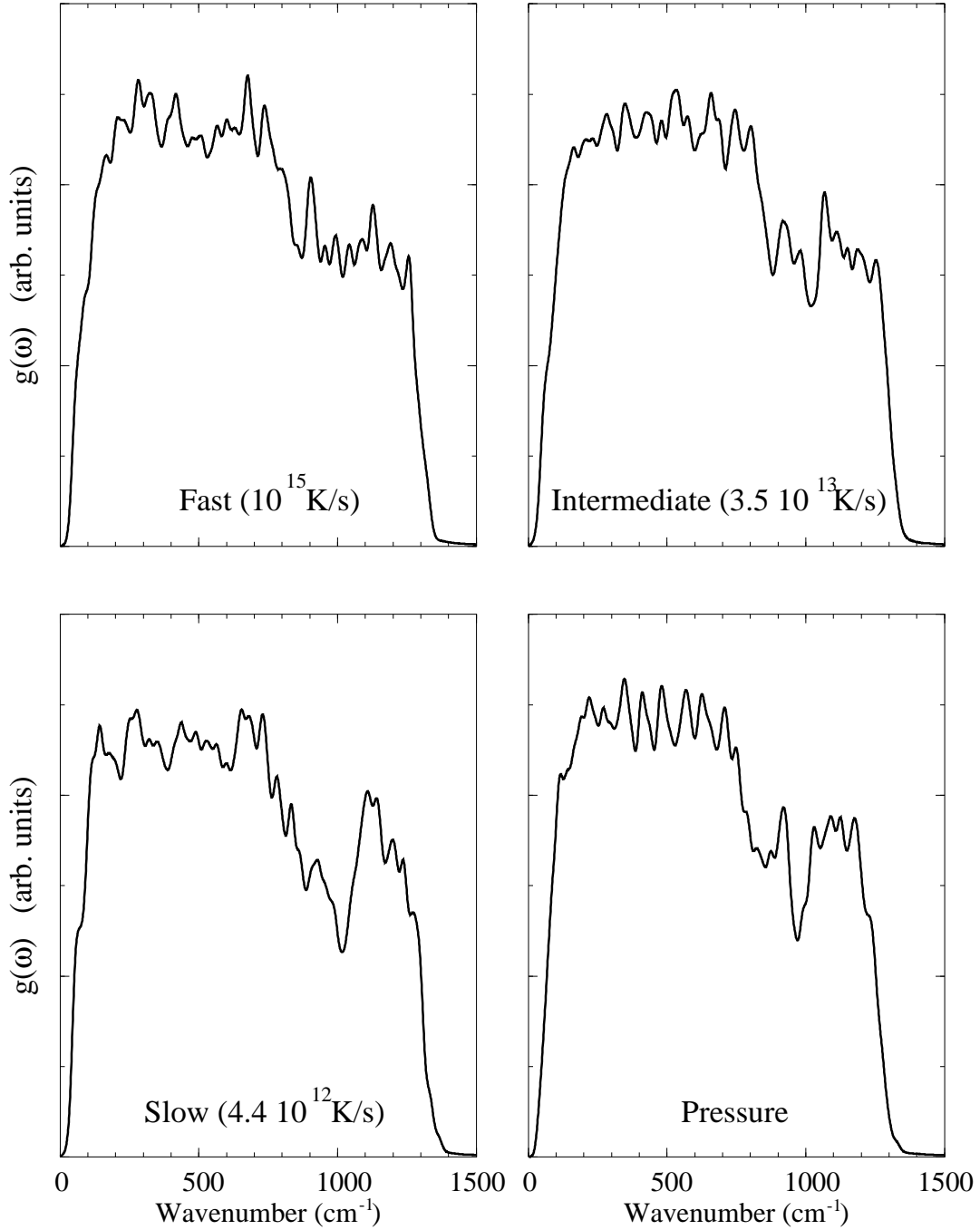


Figure 3: Vibrational densities of states for the glassy systems at $\rho = 3.07 \text{ g} \cdot \text{cm}^{-3}$ and 300 K. The three thermal glasses produced using different cooling rates are reported. Noticeable differences appear due to non-equilibrium averaging; this pseudo-dynamical quantity is very sensitive to large scale fluctuations responsible for frequency shifts in the low frequency region. It can be noticed that the rapidly cooled systems and the pressure glass are closer apart, because high-frequency stretching modes of the tetrahedron are strongly broadened in these cases. The observation of another vibrational feature at 900 cm^{-1} leads to the same conclusion.